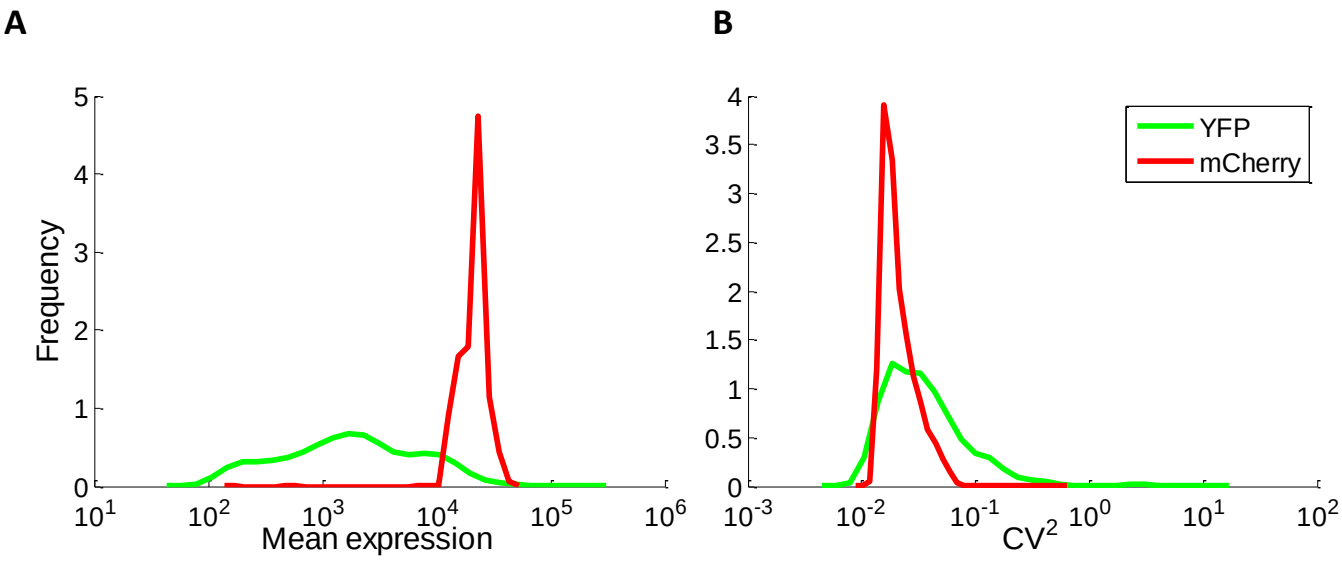

Figure S1: Distributions of YFP and mCherry mean and CV^2 for all strains

For all strains in all conditions shown is the distributions of mean (A) and noise (B) of mCherry (red) and YFP (green).

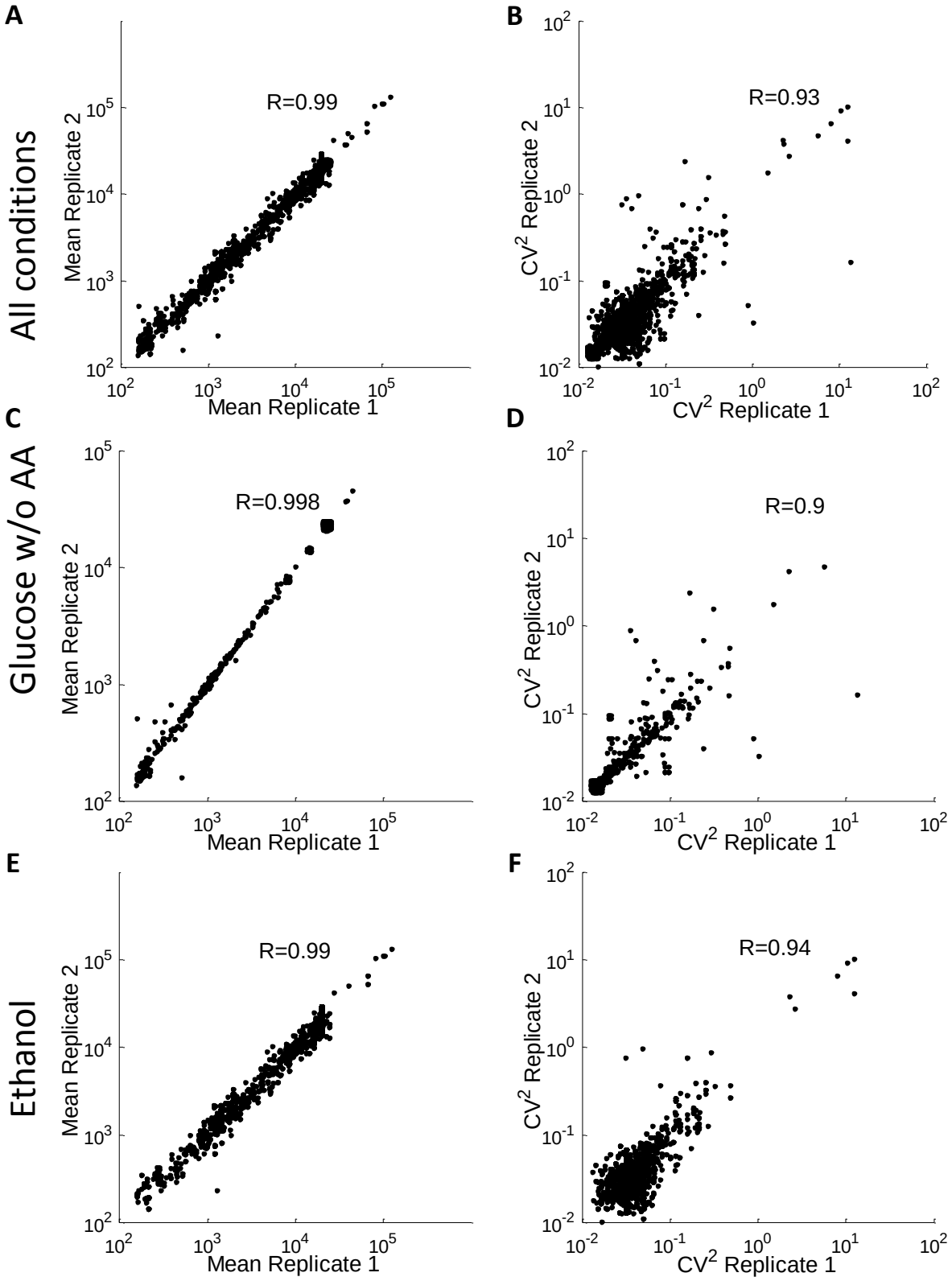

Figure S2: Replicate measurements show high reproducibility of experimental system

Reproducibility of the experimental system is assessed by biological replicates. Shown is the correlation between replicates for mean (A) and CV^2 (B) in all conditions. The reproducibility of the measurements is not affected by growth conditions, as we obtain similar correlations when examining all conditions (A,B), fast growth conditions (glucose w/o AA, C,D) or slow growth conditions (ethanol, E,F).

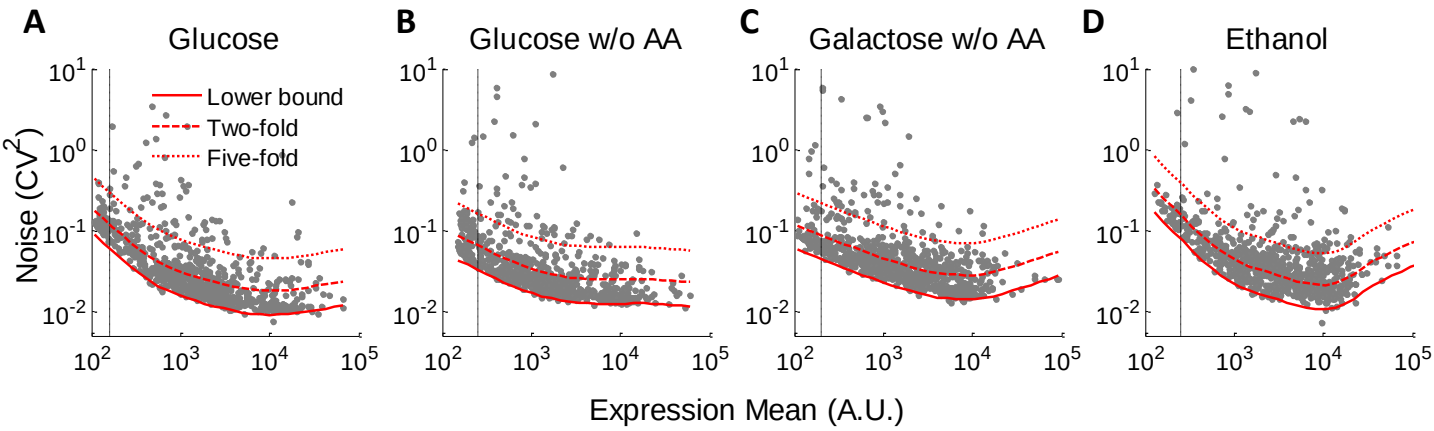

Figure S3: Mean and noise in all growth conditions

Scatter-plots of the YFP mean (x-axis) and CV^2 (y-axis) for cells grown in glucose (A), glucose w/o AA (B), galactose w/o AA (C) and ethanol (D) . Red lines depict lower noise bound (solid), 2-fold (dashed) or 5-fold (dotted) above the lower bound.

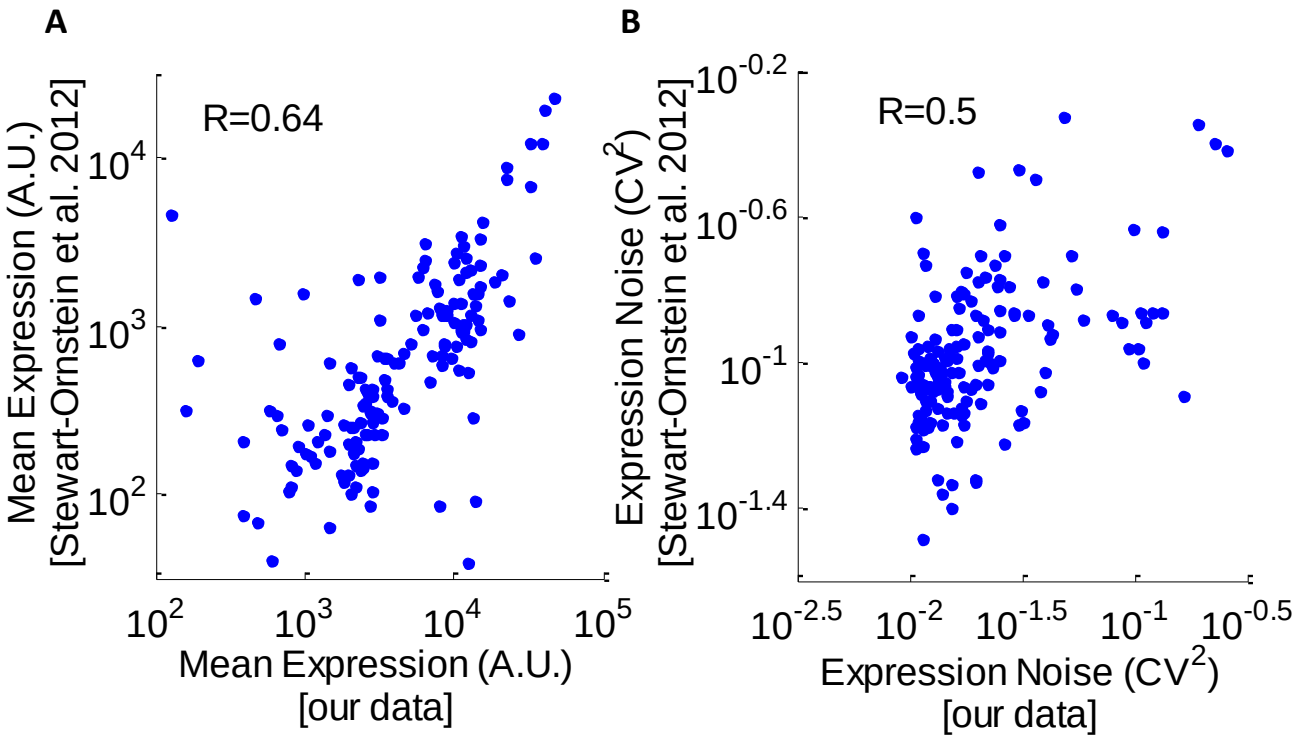

Figure S4: Promoter noise is correlated to noise in protein abundance

(A) Scatter plot of the correlations between mean expression in this study in glucose (x-axis) and published protein abundance measurements in glucose conditions from Stewart-Ornstein et al. (Stewart-Ornstein et al. 2012) (y-axis). **(B)** Same as (A) for noise.

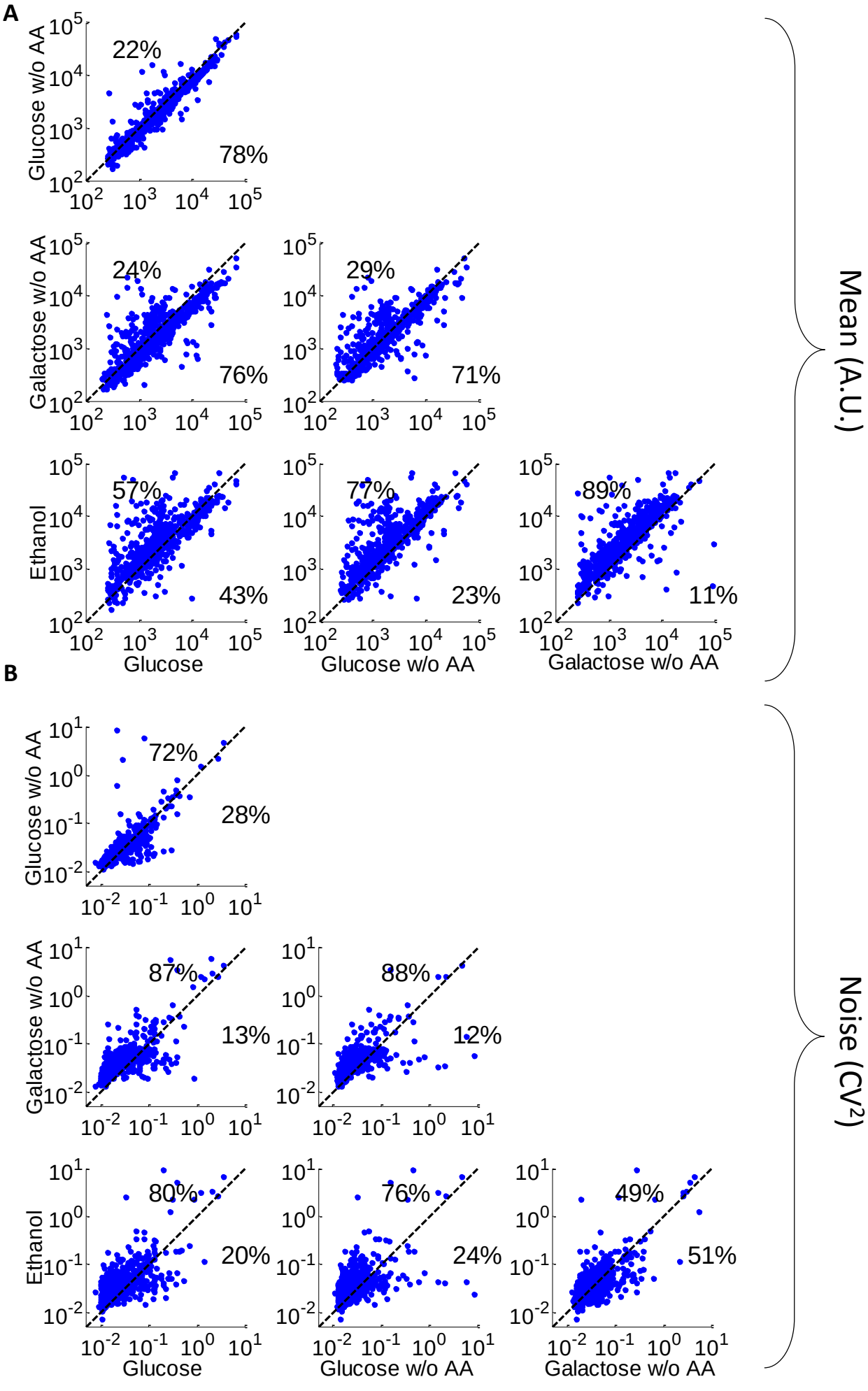

Figure S5: Global changes in mean and noise across conditions

(A) Shown is a comparison of mean YFP expression between every pair of tested conditions Dashed black line indicates Y=X. Numbers indicate percent of promoters above or below the line. **(B)** Same as (A) for noise.

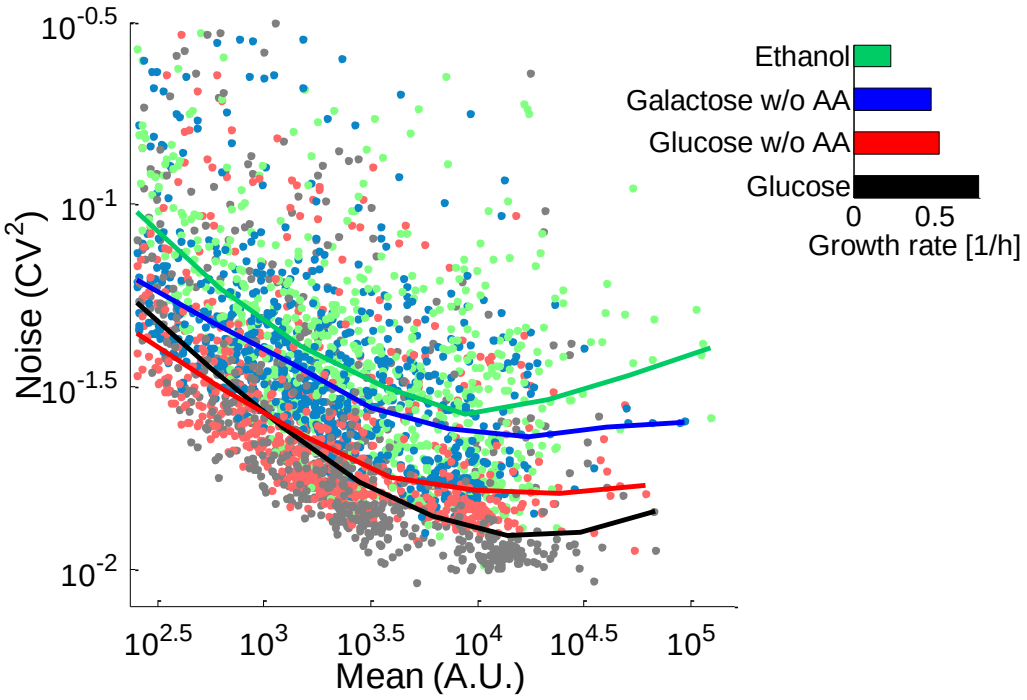

Figure S6: Noise in gene expression is higher at lower growth rates

Scatter-plot of the YFP mean (x-axis) and CV^2 (y-axis) for all promoters in each of the four conditions: Black- Glucose, Red- Glucose w/o AA, Blue-Galactose w/o AA, Green-Ethanol. For each condition a smoothed running median of the data is shown (colored lines). The different conditions exhibit different levels of noise for the same mean expression. Inset: the growth rate (in doublings per hour) in each of the tested conditions.

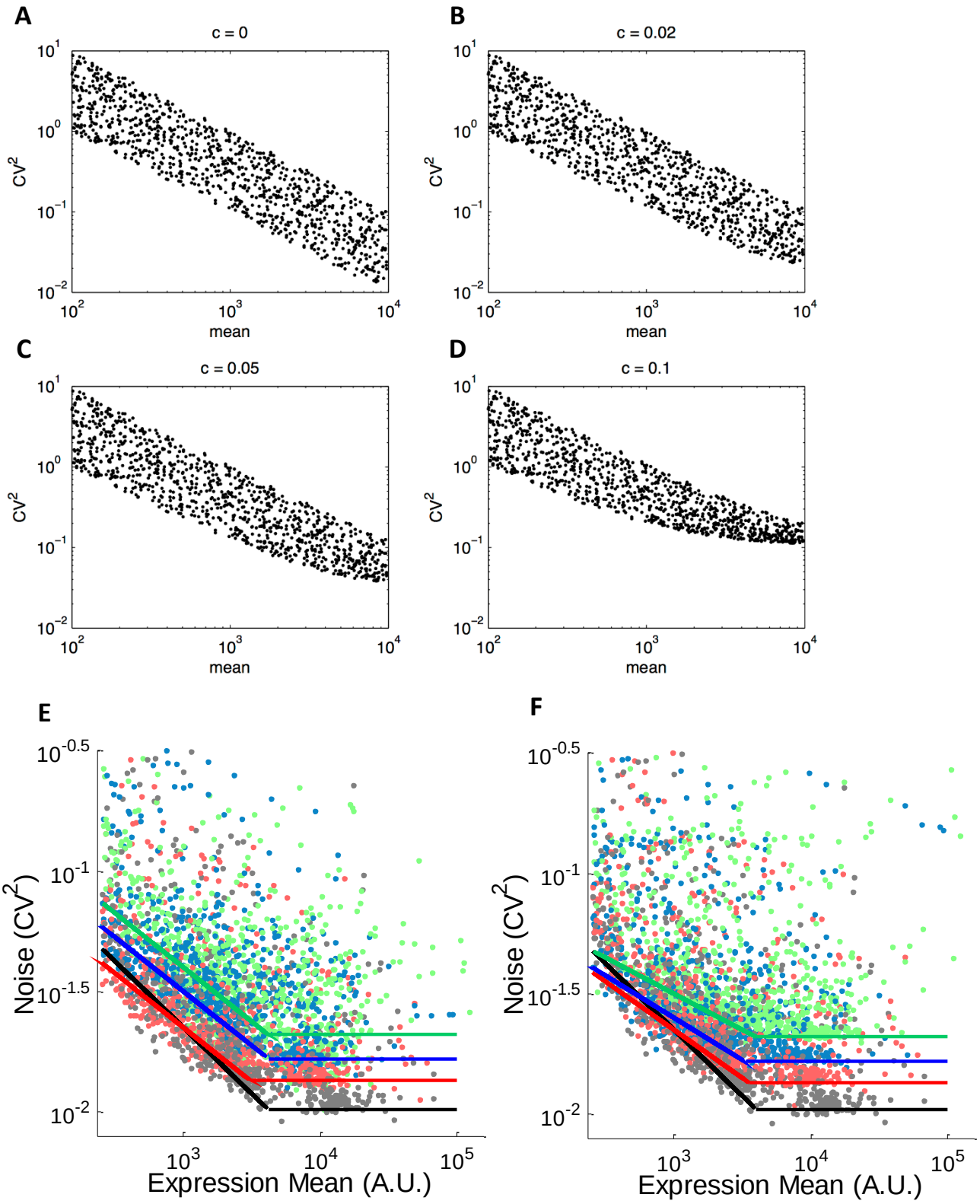

Figure S7: Increase in noise of low-expression genes is not explained by increase in extrinsic noise

(A-D) The gamma model for gene expression was used to simulate mean and intrinsic noise values. Total noise (CV^2) for each gene was then calculated as the sum of intrinsic noise and a constant extrinsic noise, ranging from 0 (A) to 0.1 (D). Changes in extrinsic noise have large effects on high-expression/low-noise genes, but only negligible effects on low-expression/high-noise genes. **(E)** Scatter-plot of the YFP mean (x-axis) and noise (CV^2, y-axis) for all promoters in each of the four conditions with linear fits of the data (same as figure 1D). Black- Glucose, Red- Glucose w/o AA, Blue-Galactose w/o AA, Green-Ethanol. **(F)** Same as in (E), but for perturbed data. For Glucose w/o AA, Galactose w/o AA, and Ethanol, noise was calculated as noise in Glucose plus the extrinsic noise limit of the condition. Mean expression for all conditions and noise in glucose remained unchanged. Lines represent linear fits to the perturbed data. While this dataset recapitulates the increase in noise for the regime of high-expression/low-noise, it underestimates the changes in noise for the regime of low-expression/high-noise.

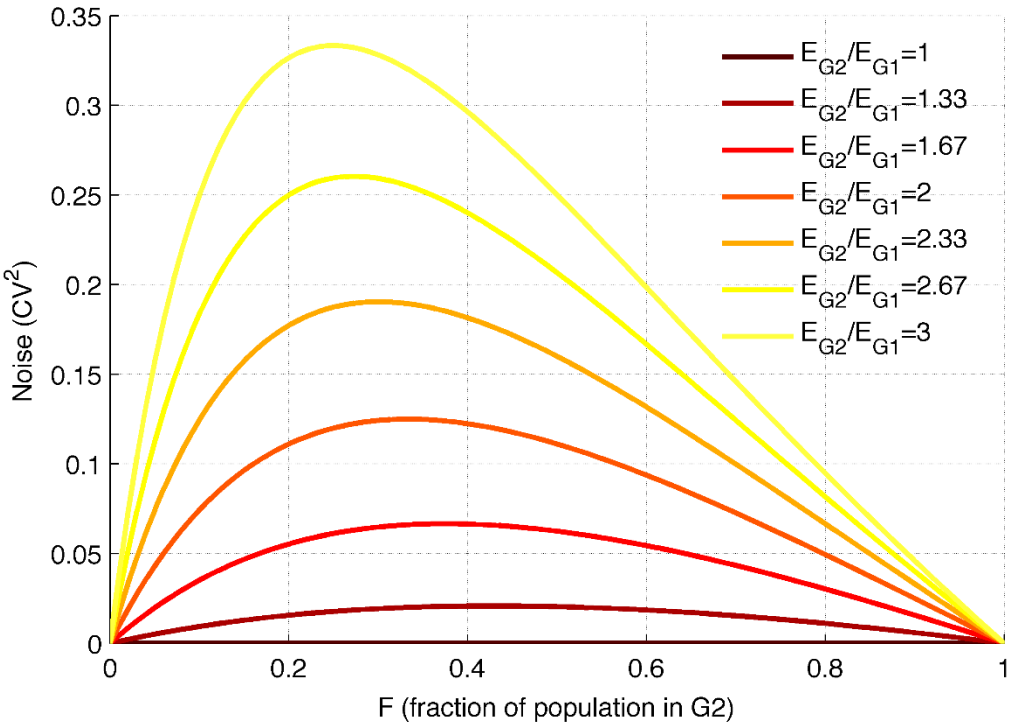

Figure S8: Cell cycle noise model predicts higher noise for larger G2/G1 expression ratios

The model prediction of how noise (CV^2 y-axis) globally changes with the G2 fraction of the population (x-axis), as in figure 2A. In this plot we do not assume that expression in G2 is twice as high as expression in G1, but rather allow it to change from 1 to 3 (colored lines). While the qualitative behavior of the curve is maintained, larger G2/G1 expression ratios result in increased noise for the same growth rate (i.e. a specific value of f).

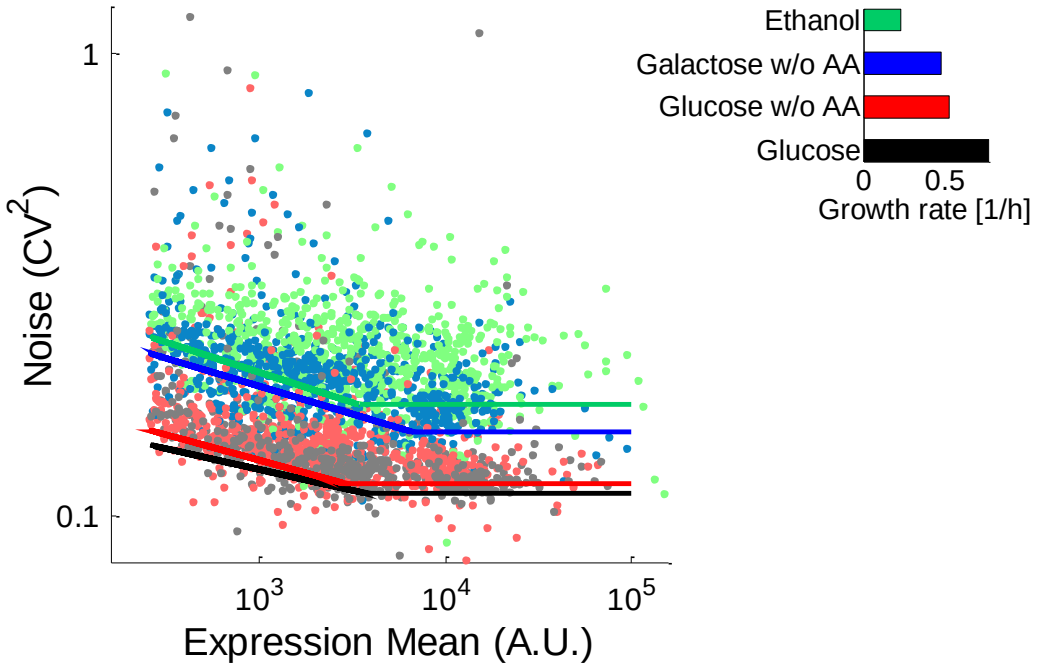

Figure S9: Noise in gene expression for cells without gating

A mild gating, by which only the most extreme 0.5% of cells in FSC and SSC were removed, was applied to all wells. Shown is a scatter-plot of the YFP mean (x-axis) and noise (CV^2, y-axis) for all promoters in each of the four conditions with linear fits of the data: Black- Glucose, Red- Glucose w/o AA, Blue-Galactose w/o AA, Green-Ethanol. The different conditions exhibit different levels of noise for the same mean expression.

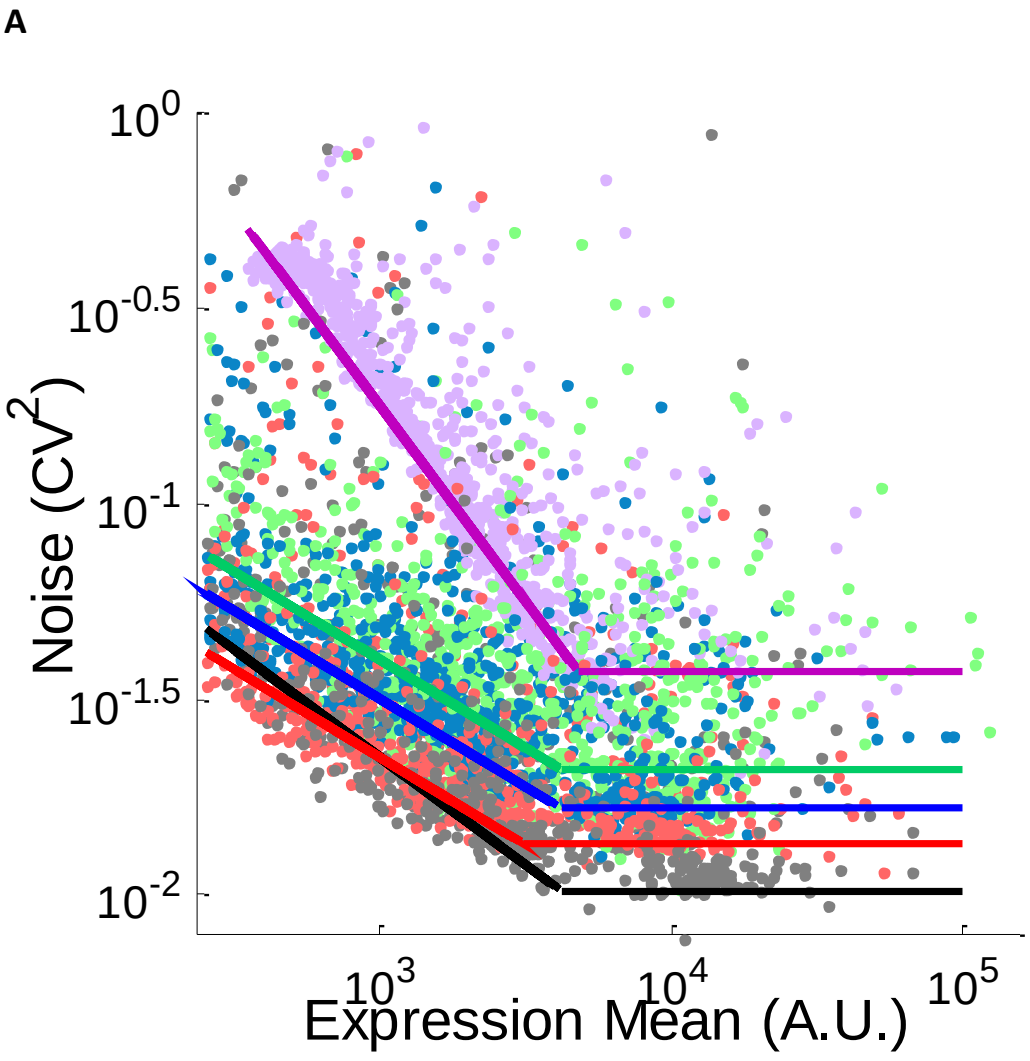

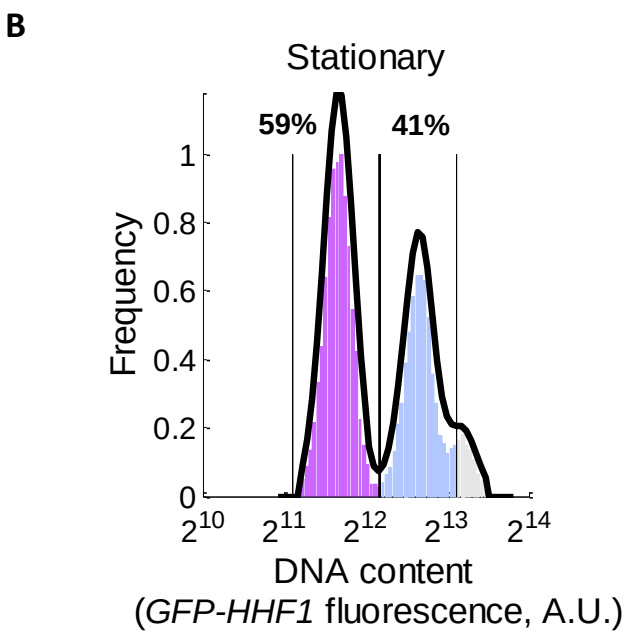

Figure S10: Noise in gene expression is higher at early stationary state

(A) Scatter-plot of the YFP mean (x-axis) and noise (CV^2, y-axis) for all promoters in each of the four conditions with linear fits of the data: Black- Glucose, Red- Glucose w/o AA, Blue-Galactose w/o AA, Green-Ethanol, Purple- early stationary phase. The different conditions exhibit different levels of noise for the same mean expression. **(B)** The fraction of G2 cells in the population at early stationary state, as determined by flow cytometry measurements of a histone reporter strain *GFP-HHF1*.

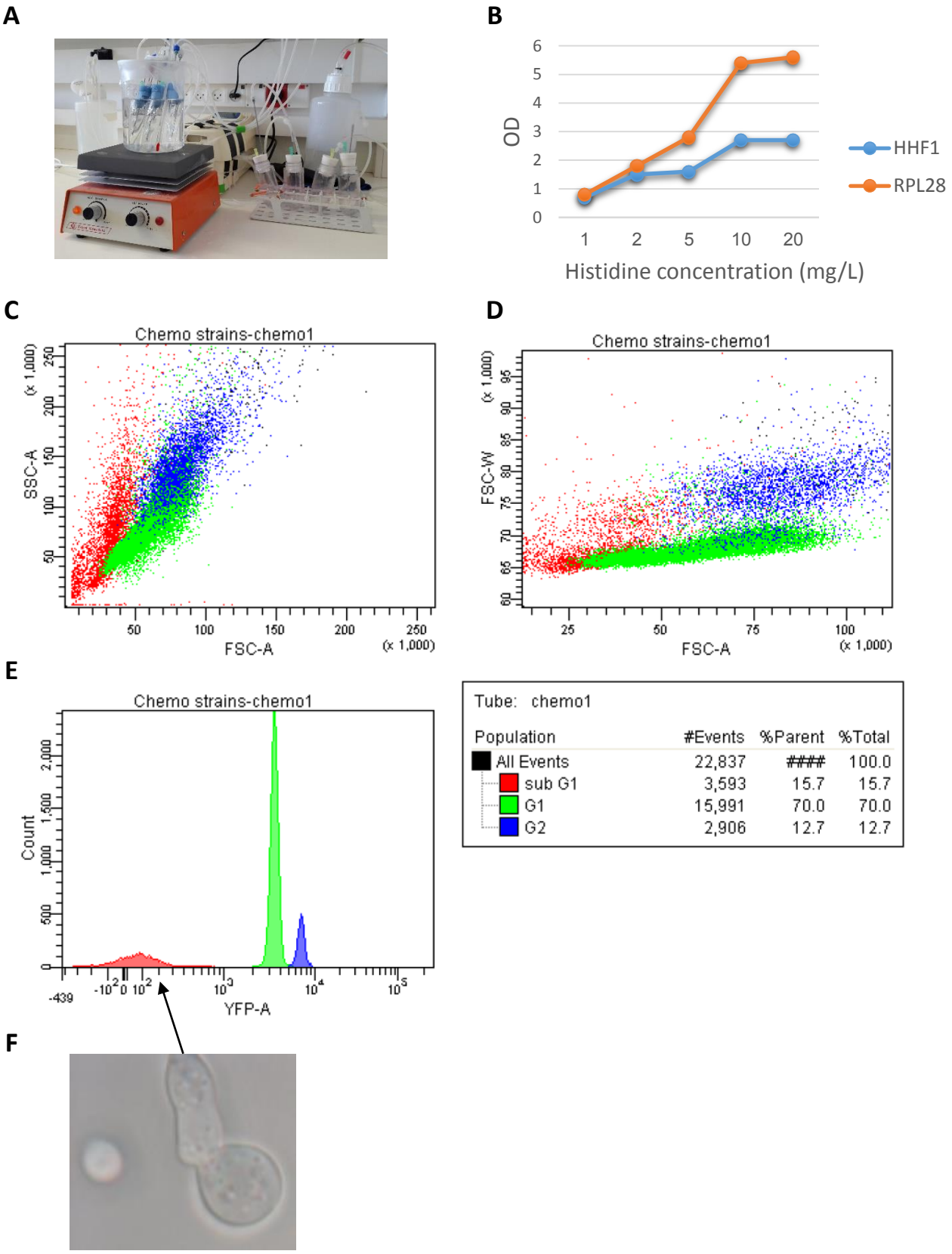

Figure S11: Noise measurements using ministat array experiments

(A) A ministat array system, allowing the growth of four strains in parallel, at a tightly controlled growth rate. **(B)** The histone reporter strain *GFP-HHF1* and the promoter reporter strain for RPL28 were grown to saturation in media with histidine concentrations raging from 1mg/L to 20mg/L as described (Brauer et al. 2008; Saldanha et al. 2004). Shown is the final OD (y-axis) as a function of the histidine in the media (x-axis). A limiting concentration of 2mg/L histidine was chosen for the chemostat experiments. **(C-E)** Flow cytometry measurements of *GFP-HHF1*grown in the chemostat at a dilution rate of $0.04h^{-1}$. Shown are different views of the cells: (A) FSC-A (x-axis) vs. SSC-A (y-axis) (B) FSC-A (x-axis) vs. FSC-W (y-axis) (C) GFP histogram. Cells were colored according to their histone content: Green- G1 (70%), Blue- G2 (13%), Red- sub-G1 (16%). Sub-G1 population is clearly distinct in FSC and SSC parameters. **(D)** Sub-G1 population is comprised of enlarged and deformed cells, and was therefore removed from further analysis.

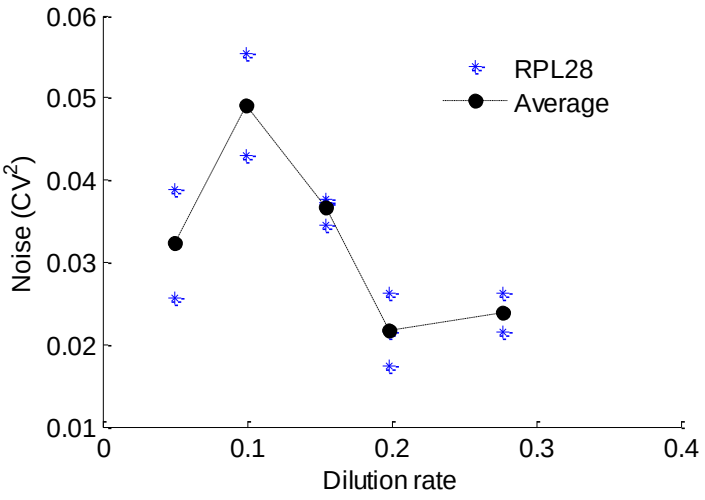

Figure S12: Noise measurements of the *RPL28* promoter in a chemostat

The promoter-reporter for RPL28 was grown in a large (100ml) histidine-limited chemostat in dilution rates ranging from $0.3h^{-1}$ to 0.05^{h-1} (corresponding to doubling times of 2 to 14 hours respectively). At each dilution rate YFP expression was measured by flow cytometry (methods). Shown is the noise (CV^2 y-axis) as a function of chemostat dilution rate (x-axis). Blue asterisks denote the measurements and black circles the average of 2-4 measurements taken at consecutive days for the same dilution rate.

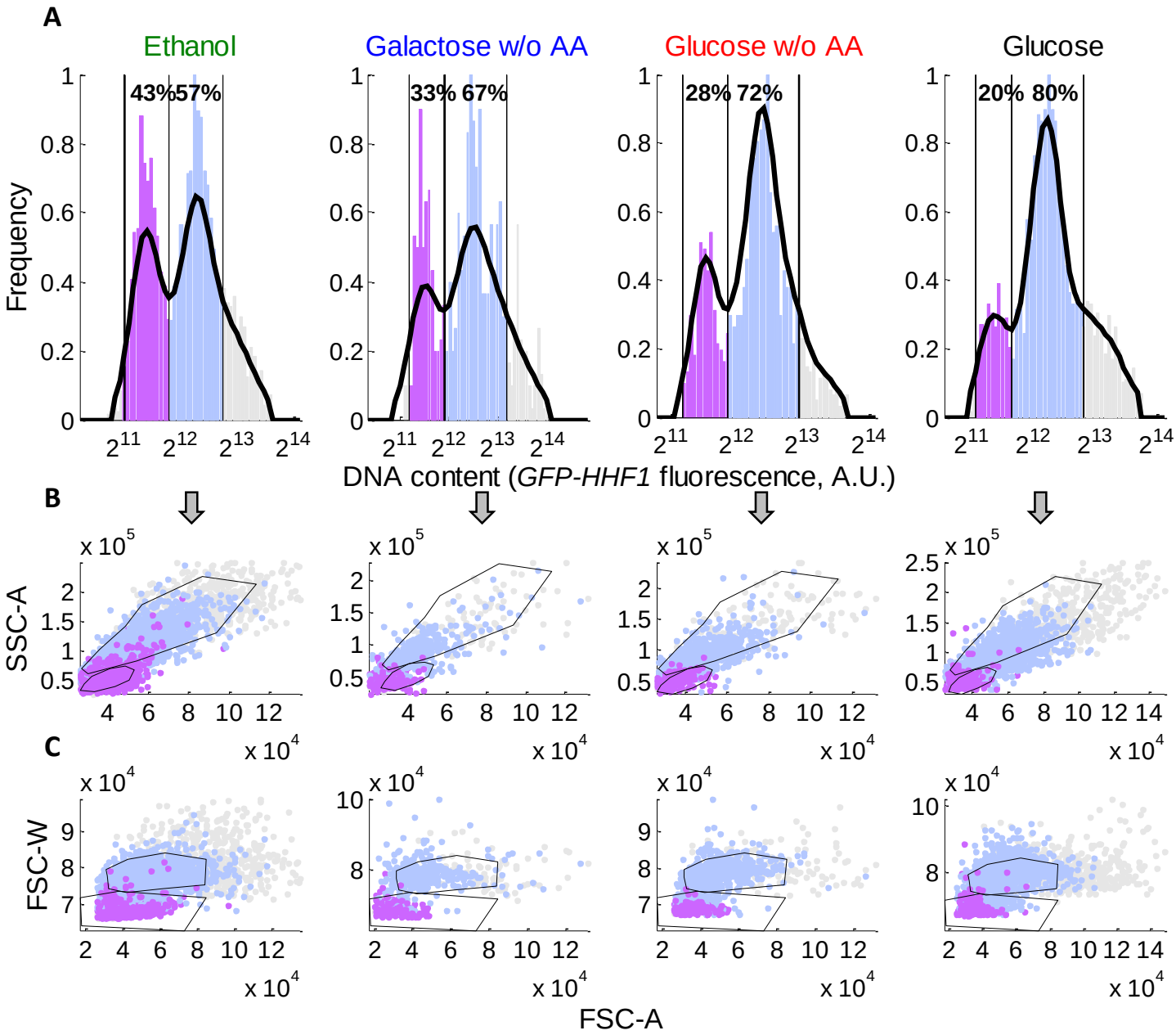

Figure S13: Extracting G1 and G2 gates on FSC and SSC from a GFP-histone strain

Based on our measurements of the histone reporter strain GFP-HHF1 **(A)**, for all conditions we generated **(B)** FSC_A-SSC_A and **(C)** FSC_A-FSC_W gates, which best separate G1 and G2 cells.

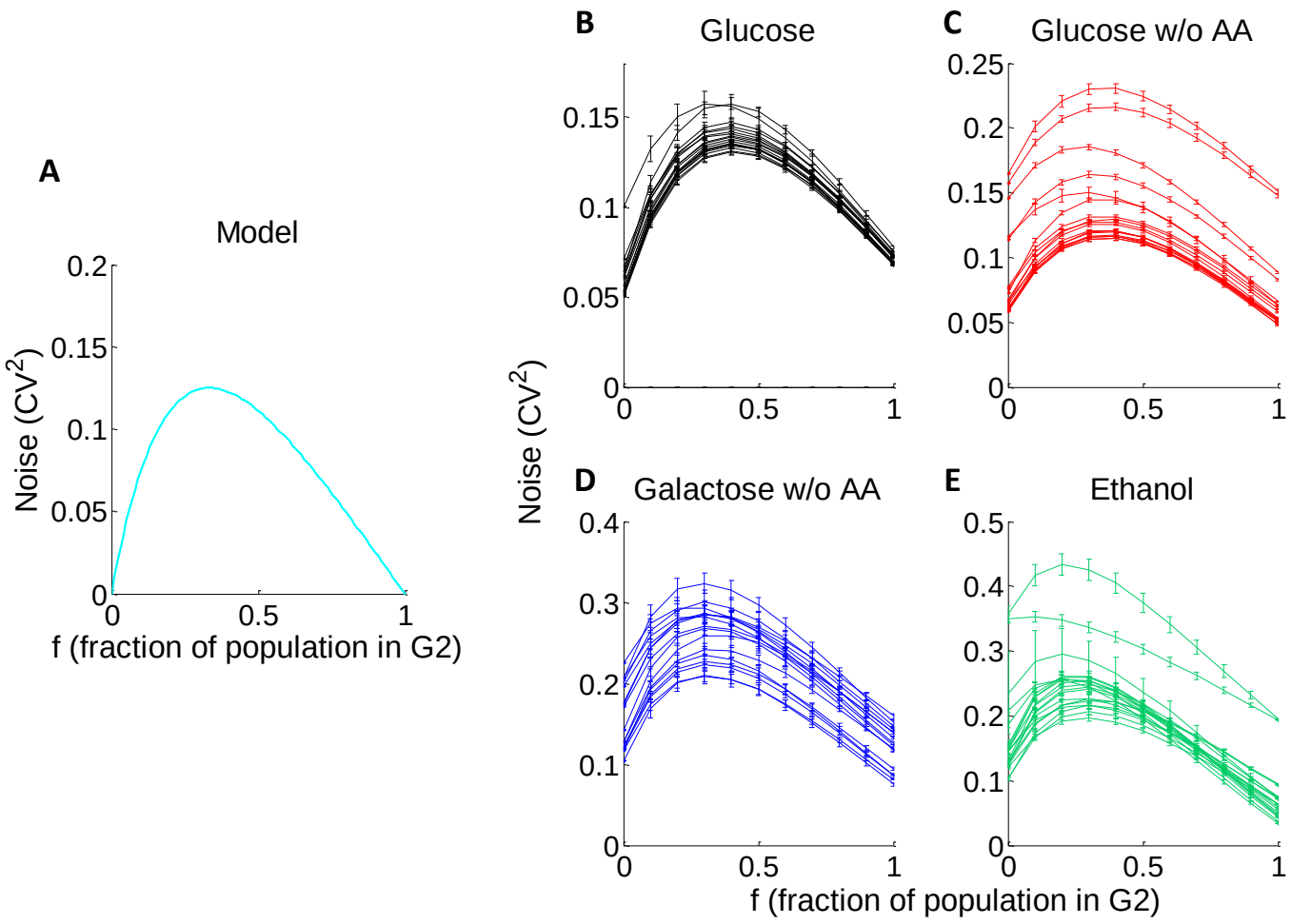

Figure S14: A model of noise that results from changes in cell-cycle stage distributions in the population predicts changes in noise for simulated wells with different G1/G2 compositions

(A) Our model prediction of how noise (CV^2 y-axis) globally changes with the G2 fraction of the population (x-axis), according to equation 1. **(B-E)** For each strain in each condition we defined cells which are most likely in G1 and G2 using our FSC-A/SSC-A and FSC-A/FSC-W gates (**fig. S12**). We randomly selected 1000 cells to generate artificial wells in-silico with predefined G2 fractions, ranging from 0 to 1. We repeated this process 500 times for each strain, and for each G2 fraction extracted the mean and std of CV^2 across all simulated wells. For 20 strains in each condition, shown are the mean and standard error of the simulated wells vs. the G2 percentages used to generate them.

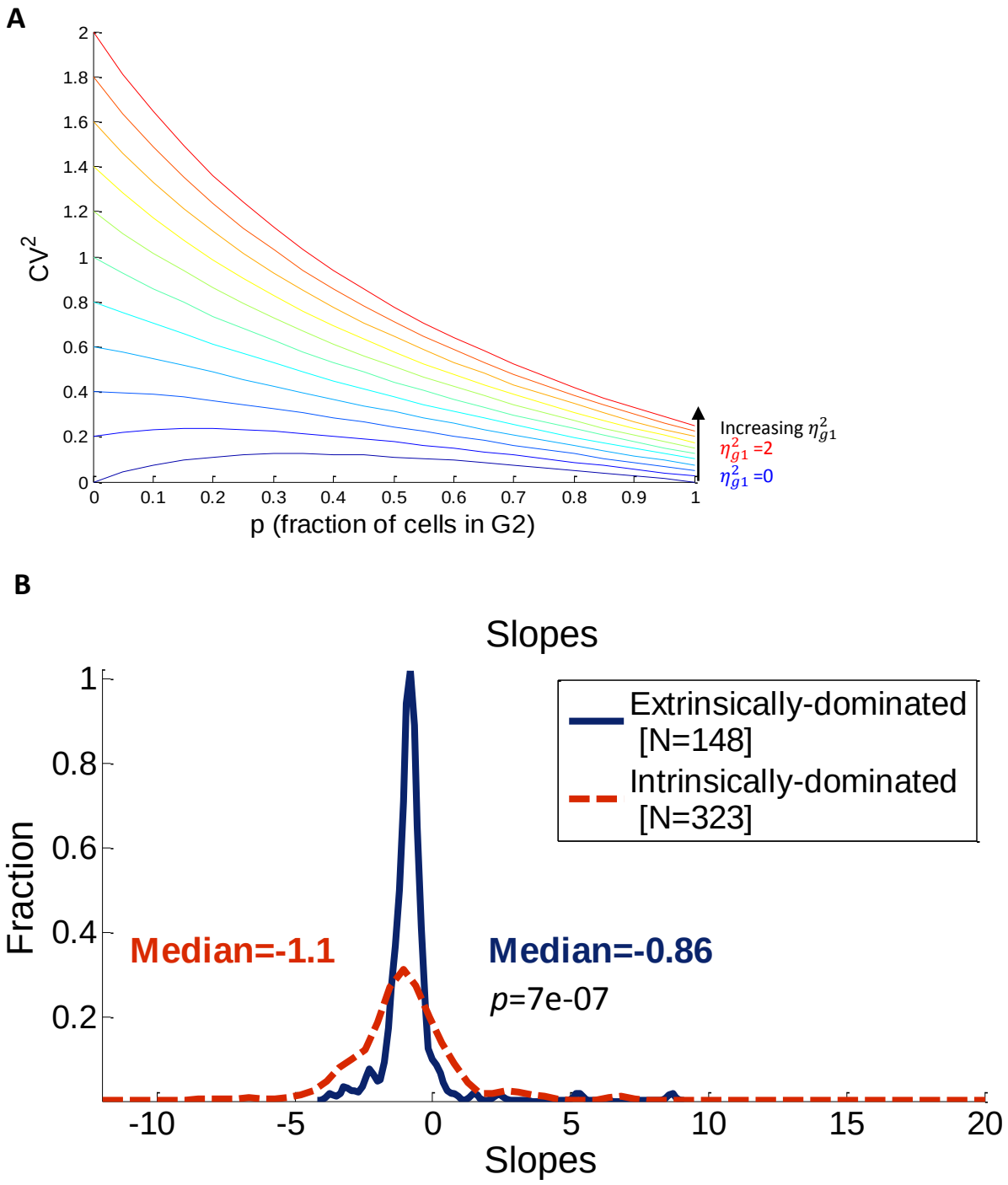

Figure S15: Promoters dominated by intrinsic noise show a larger increase in noise at lower growth-rates

(A) The model prediction of how noise (CV^2, y-axis) globally changes with the G2 fraction of the population (x-axis), for different values of η^2_{g1} according to equation 2 in the main text. Higher intrinsic noise (larger η^2_{g1}) results in a stronger decrease in noise with increasing G2 fraction. **(B)** For each gene the linear dependence between its mean and CV^2 in all growth conditions was fitted, and the slope was extracted. Shown are the distribution of slopes for two groups of genes: genes with relatively low expression (red, N=323, 38%) or high expression (blue, N=148, 17%) in all examined conditions. The variability of the low-expressing genes is dominated by the intrinsic component in all examined growth conditions (noise is significantly above the extrinsic noise limit), whereas the variability of the high-expressing genes is dominated by the extrinsic component (noise is at the limit). Intrinsically-dominated genes exhibit a significantly larger increase in noise at lower growth rates, as predicted by our model.

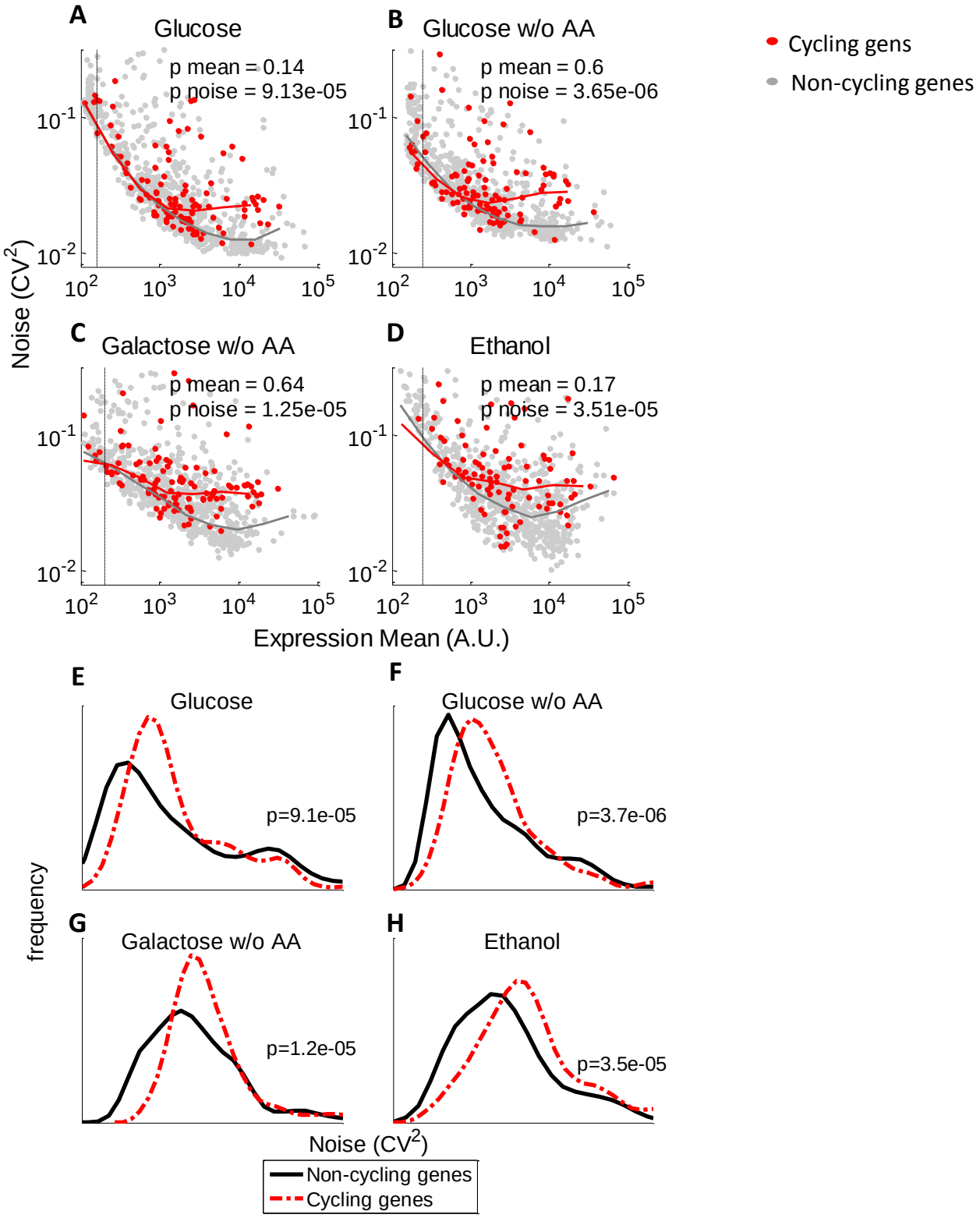

Figure S16: Cell-cycle regulated genes have higher variability levels in all growth conditions

(A) Scatter-plot of the YFP mean (x-axis) and noise (y-axis) for all promoters in glucose. Cell-cycle regulated genes (Spellman et al. 1998) are colored red. P-values are for paired K-S tests for significant differences in distributions of mean and noise. **(B-D)** Same as A, for **(B)** glucose w/o AA, **(C)** galactose w/o AA and **(D)** ethanol. **(E-H)** Noise histograms in four conditions for cycling genes (Spellman et al. 1998) (red) and non-cycling genes (black). P-values are for paired K-S tests.

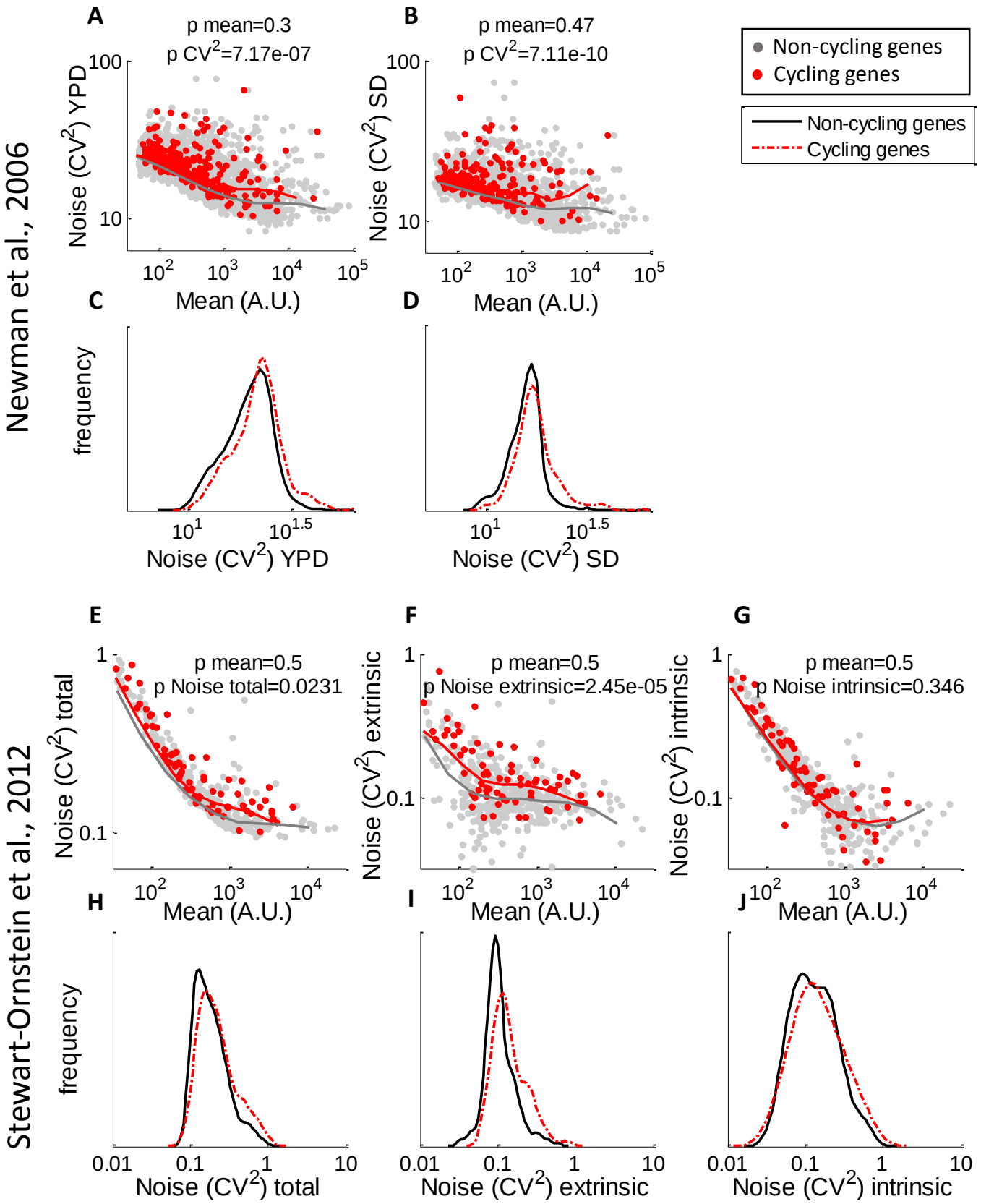

Figure S17: Cell-cycle regulated genes have higher variability levels in protein-abundance datasets

(A-B) Scatter-plot of the YFP mean (x-axis) and noise (y-axis) for protein abundances taken from Newman et al. (Newman et al. 2006) for yeast grown in either YPD (A) or SD (B). Cell-cycle regulated genes (Spellman et al. 1998) are colored red. P-values are for paired K-S tests for significant differences in distributions of mean and noise. **(C-D)** Noise histograms for the data shown in (A) and (B) respectively. **(E-G)** Same as in A, for data taken from Stewart-Ornstein et al. (Stewart-Ornstein et al. 2012). In this dataset total noise (E) was decomposed to extrinsic noise (F) and intrinsic noise (G) (Stewart-Ornstein et al. 2012). We find that cell-cycle regulated genes show increased extrinsic noise, as predicted by our model. **(H-J)** Noise histograms for the data shown in (E), (F) and (G) respectively.

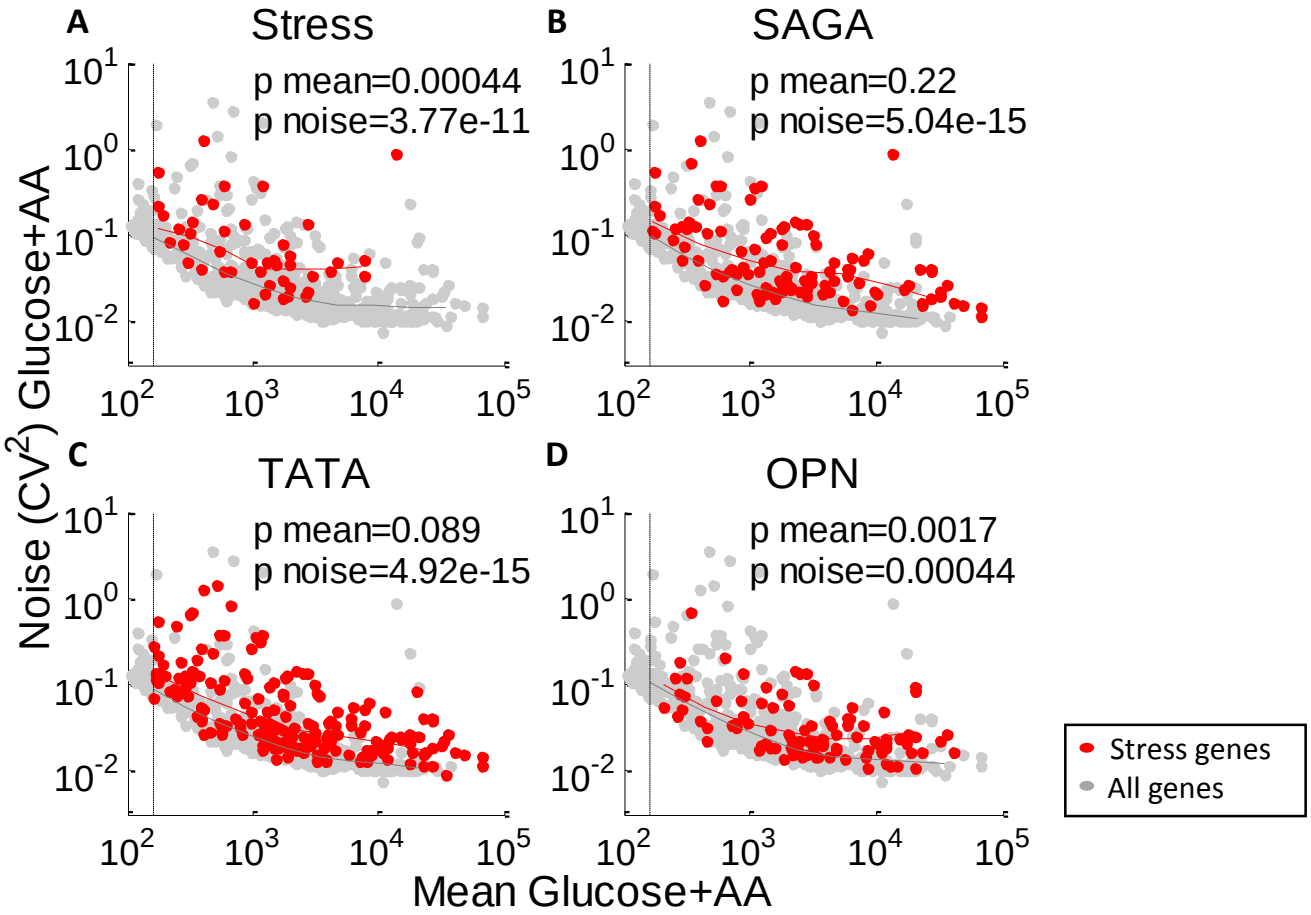

Figure S18: Features correlated with high noise in rich growth conditions

(A) Scatter-plot of the YFP mean (x-axis) and noise (y-axis) in glucose. Genes upregulated in stress (Gasch et al. 2000) are colored red. P-values are for paired K-S tests for significant differences in mean and noise. **(B)** Same as (A), highlighting promoters predominantly regulated by SAGA (Huisinga and Pugh 2004) . **(C)** Same as (A), highlighting promoters with a strong TATA (Basehoar et al. 2004). **(D)** Same as (A), highlighting promoters with a well-positioned -1 nucleosome (Tirosh and Barkai 2008).

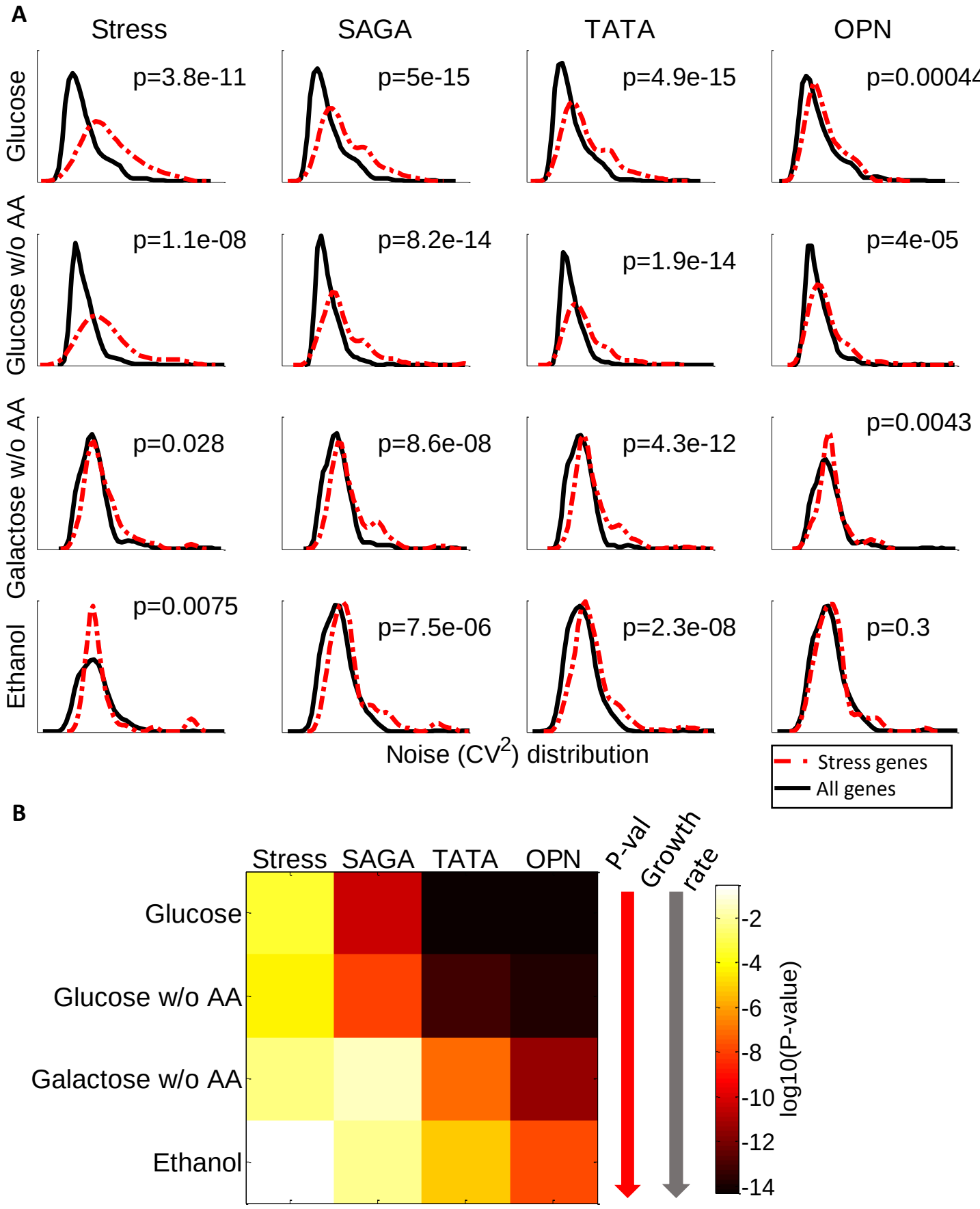

Figure S19: Features associated with high noise decrease in significance with at lower growth rates

(A) Noise histograms in all conditions for all genes (black) or a specific group (red). Groups are as in figure S11. P-values are for paired K-S tests. **(B)** Heat map of the K-S p-values from (A). For all features, p-values decrease with decreasing growth rate.

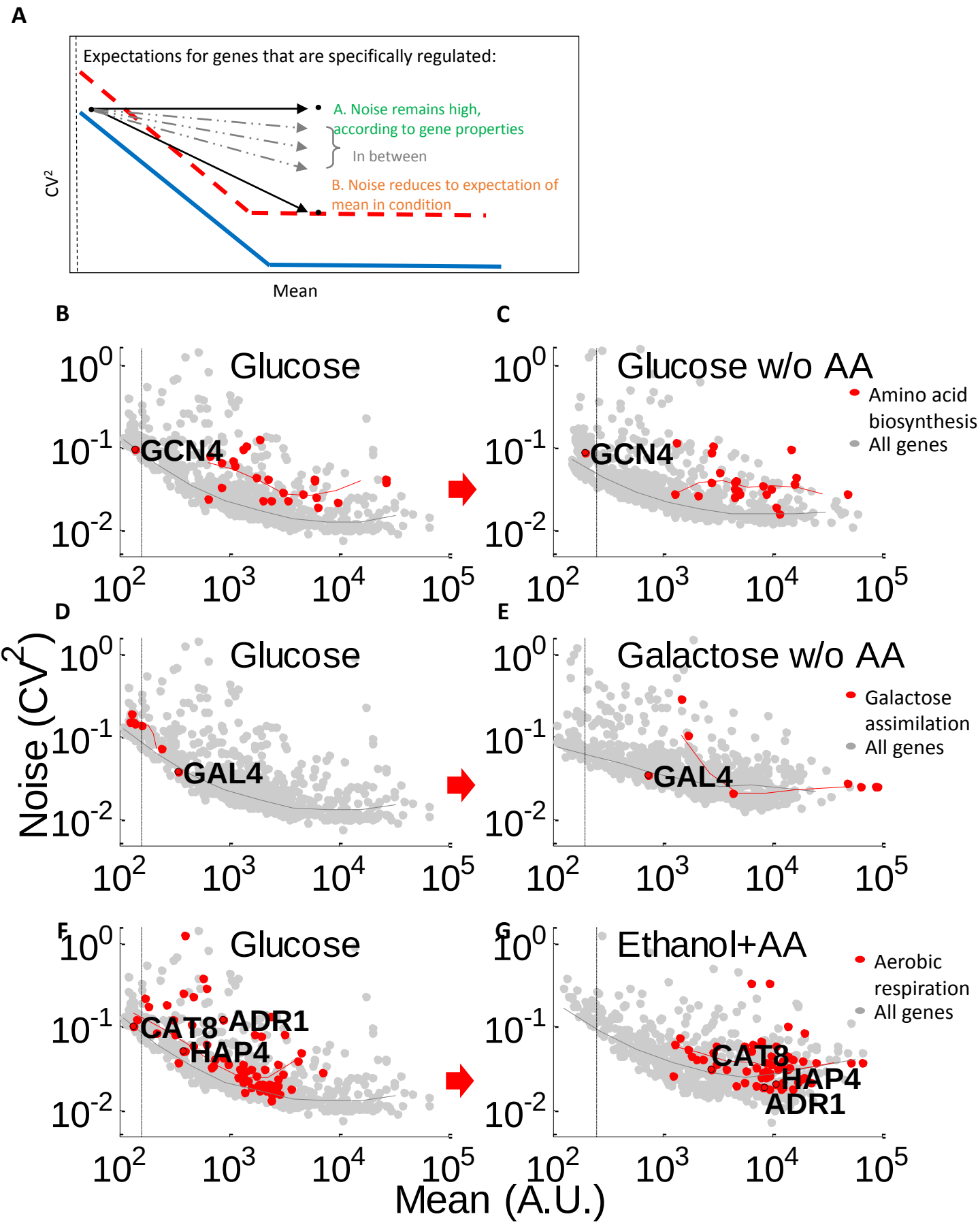

Figure S20: Noise of specifically-regulated gene groups is associated with regulator noise

(A) Schematic illustration for how the noise of an upregulated gene (black dot) is expected to behave when changing growth conditions. Curves represent the average population mean and noise in either fast (blue) or slow (red) growth conditions. **(B-C)** Scatter-plot of the YFP mean (x-axis) and noise (y-axis) for all promoters (gray) grown in glucose either with amino acids (B) or without (C). Amino-acid biosynthesis genes, previously determined to be up-regulated in glucose-AA (Keren et al. 2013) are highlighted in red. When repressed the amino acid biosynthesis genes have high levels of noise. High noise (higher than expected by the mean expression of the genes) is preserved when the group is upregulated, in accordance with the high noise of the group's master regulator- *GCN4*. **(D-E)** Same as (B-C), but highlighting the galactose assimilation genes, differentially regulated between growth on glucose (D) and galactose (E). Activated genes have noise levels comparable to the expectation from their mean expression, in accordance with the low noise of the group's master regulator- *GAL4*. **(F-G)** Same as (B-C), but highlighting aerobic respiration genes, differentially regulated between growth on glucose (G) and ethanol (G). Activated genes have noise levels comparable to the expectation from their mean expression, in accordance with the low noise of the group's master regulators- *HAP4*, *CAT8* and *ADR1*.

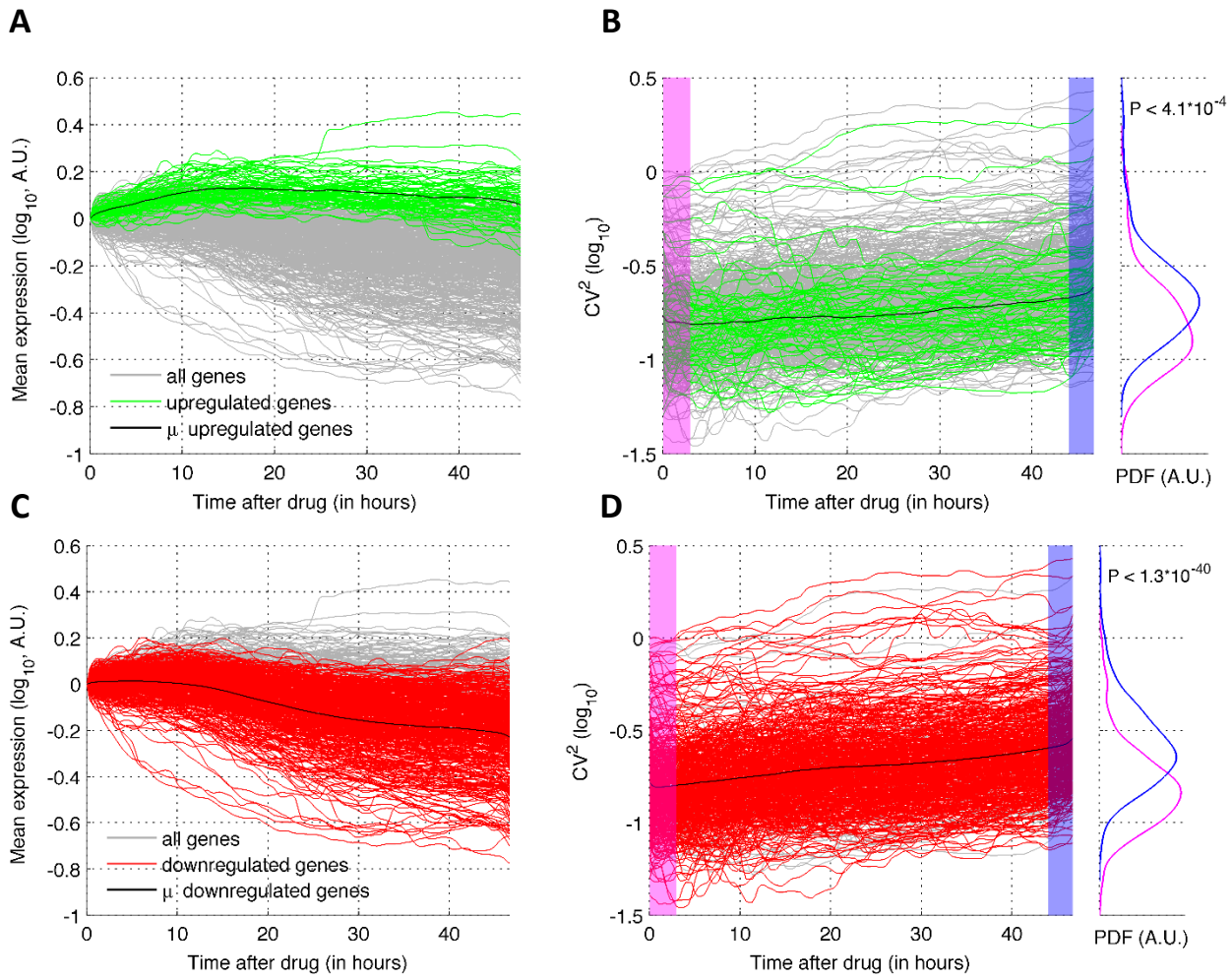

Figure 21: Protein abundance variability in cancer cells globally increases in response to a drug

Time-lapse microscopy data of 542 fluorescently tagged proteins in individually tracked cancer cells in response to a drug (Cohen et al. 2008b). Shown is the mean protein abundance (A,C) and noise in protein abundance (B,D), for all genes (gray lines), genes whose mean abundance increases in response to the drug (highlighted by green lines in A) and genes whose mean abundance decreases in response to the drug (red lines, B). After drug addition cell-to-cell variability increases significantly for most proteins, including upregulated (green lines, C) and down-regulated genes (red lines, D). Histograms (B,D) represent the noise distributions of either upregulated (B) or down-regulated (D) genes at the start (pink) or the end (blue) of the experiment. P-values are for paired K-S test.